Journal of
Applied Crystallography
ISSN 0021-8898

Received 16 August 2006
Accepted 27 January 2007

Fractal aggregates of the Pt nanoparticles synthesized by the polyol process and poly(*N*-vinyl-2-pyrrolidone) reduction

Jhih-Min Lin,[a] Tsang-Lang Lin,[a]* U-Ser Jeng,[b]* Yu-Jen Zhong,[c] Chuin-Tih Yeh[c] and Tsan-Yao Chen[a]

[a]Department of Engineering and System Science, National Tsing Hua University, Hsinchu 300, Taiwan, [b] National Synchrotron Radiation Research Center, Hsinchu 300, Taiwan, and [c]Department of Chemistry, National Tsing Hua University, Hsinchu 300, Taiwan. Correspondence e-mail: tllin@mx.nthu.edu.tw, usjeng@nsrrc.org.tw

Small-angle X-ray scattering was used to characterize the size and aggregation behavior of the Pt nanoparticles synthesized by the polyol process and the unusual poly(*N*-vinyl-2-pyrrolidone) (PVP) reduction. With formaldehyde (HCHO) as the reduction agent, the Pt nanoparticles synthesized in aqueous solutions with a high PVP/$PtCl_4$ weight ratio were characterized by short rods with a 70% polydispersity in rod length. The size and size distribution of the rod-like Pt nanoparticles (3 nm in rod length and 2 nm in rod diameter) are consistent with the corresponding transmission electron microscopy image. With a comparable PVP/$PtCl_4$ weight ratio in the aqueous solution containing HCHO, the high number density of reduced Pt nanoparticles led to a fractal-like aggregation with a fractal dimension of 2.1 and a correlation length of ~30 nm. We also demonstrated that Pt nanoparticles can be synthesized by PVP reduction at 323 K without HCHO. The particle size and the clustering behavior of the Pt nanoparticles reduced by PVP are closely related to the PVP concentration in the solution. Both the Pt nanoparticles synthesized in the commonly used polyol process and the unusual PVP reduction form fractal-like clusters *via* the PVP–metal nanoparticle association when the number density of the Pt nanoparticles in the solutions is high.

1. Introduction

The polyol reduction process is often employed in the synthesis of nanometre-sized metallic particles (Chen *et al.*, 2002). In the polyol process, metal precursors undergo chemical reduction in solutions containing polyols (such as ethylene glycol) and organic capping agents such as cetyltrimethylammonium bromide (CTAB) or poly-vinylpyrrolidone (PVP). The resulting metal nanoparticles can have well controlled size and shape (Murphy & Jana, 2002; Sun *et al.*, 2002). The size and size distribution are especially critical when the metal particles are to be used as catalysts, such as Pt and Pt-based alloyed nanoparticles in the electrodes of direct methanol fuel cells (Nam *et al.*, 2004; Hogarth & Ralph, 2002; Joo *et al.*, 2001; Liu *et al.*, 2000). For electrode applications, keeping a good dispersion (less aggregation) of the metal nanoparticles synthesized is important (Joo *et al.*, 2001), as is small size, 1–3 nm, for large surface areas (Camara *et al.*, 2002).

In the structural characterization of nanoparticles in colloidal solutions, small-angle X-ray scattering (SAXS) is advantageous due to the sensitivity to nanostructure and the flexibility in sample environment (Chen & Lin, 1987). The latter is especially important in *in-situ* measurements for structural evolution. In this study, we employ SAXS to study the structural information, including size, shape, aggregation, and structural evolution, of the Pt nanoparticles synthesized by the polyol process (Hashimoto *et al.*, 1998) and by an unusual PVP reduction. PVP is often used as an agent to protect the metal nanoparticle synthesized in the polyol process from aggregation. Nevertheless, we found here that simply by elevating the temperature of an aqueous solution containing $PtCl_4$ and PVP, Pt nanoparticles can be reduced from the solution due to the weak reduction capability of PVP at the elevated temperature. Below, we detail the use of SAXS in extracting the structural characteristics of the Pt nanoparticles in the solutions in which they are synthesized.

2. SAXS model

For a fractal system formed by the aggregation of primary particles in a self-similar geometrical arrangement, the mass of the system increases with its linear dimension r according to $M \propto r^D$ (Freltoft *et al.*, 1986). The exponent D can be a non-integer value between 1 and d, where d is the Euclidean dimension. Contrary to condensed-matter systems where D is the same as d, the fractal dimension of, for example, aggregates of fine silica particles of a porous structure is often found to be between 2 and 3 (Schmidt, 1991), whereas D is 2 for polymer networks with Gaussian chain conformations (Higgins & Benoit, 1994). From the mass–dimension relation, $M \propto r^D$, a pair correlation function

$$g(r) \propto r^{D-d} \exp(-r/\xi) \quad (1)$$

can be constructed for a fractal system (Mangin *et al.*, 1985). In this equation, an exponential cutoff is imposed through the correlation length ξ which accounts for the finite size of the fractal region (~2ξ) of the system.

The corresponding SAXS intensity for a fractal system can be expressed as $I(Q) \propto P(Q)S(Q)$, where

$$S(Q) = 1 + \frac{1}{(QR)^D} \frac{D\Gamma(D-1)}{[1+(Q\xi)^{-2}]^{(D-1)/2}} \sin[(D-1)\tan^{-1}(Q\xi)] \quad (2)$$

and can be obtained from the Fourier transform of equation (1) (Chen & Teixeira, 1986; Guo *et al.*, 1990), where R is the radius of the primary particles. The modulus of the scattering vector $Q = (4\pi/\lambda)\sin(\theta/2)$ is defined by the scattering angle θ, and the wavelength of the X-rays λ. For small particles with normalized values of $P(Q) \simeq 1$ for the range of Q of interest, the scattering profile $I(Q) \propto Q^{-D}$ is dominated by the power-law scattering behavior in the Q region where $Q\xi >> 1$ (Freltoft *et al.*, 1986). On the other hand, sphere-, ellipsoid-, and rod-like form factors are often employed in the SAXS data analysis for colloidal solutions (Chen & Lin, 1987). Analytical formulae for these form factors with polydispersity in size (for instance, using a Schultz distribution for sphere radius or rod length) have been discussed in detail in the literature (Sheu, 1992).

3. Experiment

Pt nanoparticles were mainly synthesized *via* the polyol process with the reduction agent formaldehyde (HCHO) and the aggregation protection agent poly(*N*-vinyl-2-pyrrolidone) (PVP, $M_w \simeq 10\,000$) in aqueous solutions with a pH value of 12 obtained using NaOH (for a higher reduction potential of HCHO). The Pt nanoparticles formed in two sample solutions (1) and (2) were studied by collecting SAXS data on the original reduction solutions. Solution (1) was an aqueous solution with 16 mg ml^{-1} PVP, 1 mg ml^{-1} $PtCl_4$, and excess HCHO, and solution (2) was an aqueous solution with 16 mg ml^{-1} PVP, 10 mg ml^{-1} $PtCl_4$, and excess HCHO. Another sample solution with 25 mg ml^{-1} $PtCl_4$ and 40 mg ml^{-1} PVP was prepared without HCHO. The yellowish solution of PVP/$PtCl_4$, reflecting mainly the color of $PtCl_4$, stayed stable for weeks at room temperature, and was then placed in an oven at 323 K. After 72 h of incubation, an isotropic black solution was obtained, indicating the formation of Pt nanoparticles.

SAXS measurements were conducted on the 8 m SAXS instrument at the National Tsing-Hua University, Hsinchu, Taiwan. The X-ray beam emitted from the 18 kW rotating anode (copper target) was monochromated by pyrolytic graphite to a wavelength of 1.54 Å, and collimated by three pinholes arranged over 3 m for a beam of 1 mm diameter. Sample solutions were sealed in a copper sample cell with two thin Kapton sheets for X-ray windows. With a sample-to-detector distance of 4.1 m, the SAXS data measured by the area detector covered a Q range from 0.01 to 0.2 Å^{-1}. All the SAXS data were corrected for sample transmission, background, and detector sensitivity, and normalized to the absolute scattering scale, namely, scattering cross section per unit sample volume $I(Q)$.

4. Results and discussion

4.1. Pt nanoparticles synthesized with a high PVP/$PtCl_4$ weight ratio

Fig. 1 shows the Kratky–Porod plot of the SAXS results for the Pt nanoparticles in the well aggregation-protected PVP solution. With the high PVP/$PtCl_4$ weight ratio of 16, the SAXS data measured for the sample solution show no sign of aggregation. The SAXS data measured for the successively diluted sample solutions of 0.5C, 0.25C, and 0.0625C of the PVP concentration C (= 16 mg ml^{-1}) at a fixed PVP/$PtCl_4$ weight ratio of 16 indicate that the small interactions of the Pt nanoparticles can be largely eliminated by the dilution of sample concentration. All the four sets of data can be fitted by the Kratky–Porod approximation (straight lines in the inset of Fig. 1) with a common rod radius of 9.8 ± 0.2 Å, revealing a stable rod-like characteristic for the Pt nanoparticles.

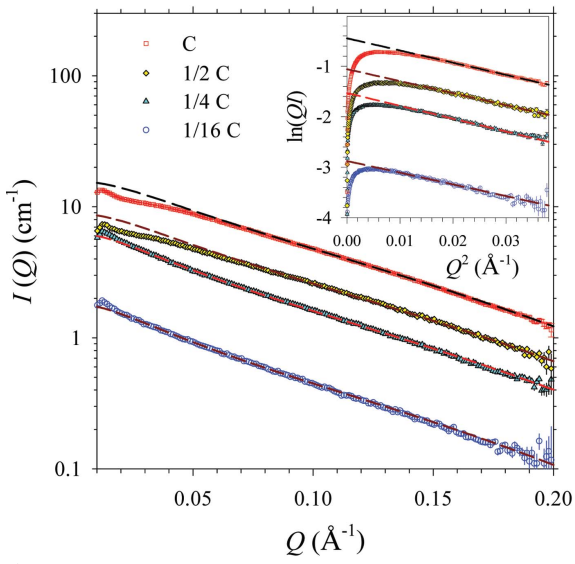

Figure 1
SAXS data for the Pt nanoparticles in the aqueous solutions of PVP concentrations of 1C, 0.5C, 0.25C, and 0.0625C (1C = 0.016 mg ml^{-1}), and a fixed $PtCl_4$/PVP weight ratio of 1/16. The data are fitted (dashed curves) using a rod-like model. The inset shows the corresponding data fitted (dashed lines) with the Kratky–Porod approximation.

We modeled the SAXS data for the Pt nanoparticles using a rod-like form factor with a Schultz distribution in rod length. The analytical form of the polydisperse rod form factor involves the fitting parameters of rod radius, averaged rod length, and polydispersity in the rod length (Sheu, 1992). Fig. 1 shows the model fitting results for the SAXS data. Except for the small deviations in the low-Q region of the two sets of data for higher Pt nanoparticle concentrations (1C and 0.5C), these four sets of data can be well described by the polydisperse rod model, with the same common parameters of a most-probable rod length of 3.0 nm, a polydispersity of 70% in rod length, and a rod radius of 1.0 ± 0.1 nm (Fig. 2). The mean rod length for the relatively large length distribution of the rods is 6.0 ± 0.5 nm. The most probable rod length of the Pt nanoparticles extracted from the SAXS data is essentially consistent with that observed in the transmission electron microscopy (TEM) image (inset of Fig. 2).

4.2. Pt nanoparticles synthesized with a comparable PVP and $PtCl_4$ weight ratio

Fig. 3 shows the SAXS data for the Pt nanoparticles synthesized in the aqueous solution of 16 mg ml^{-1} PVP and 10 mg ml^{-1} $PtCl_4$. The SAXS data show a characteristic power law scattering of $I \propto Q^{-D}$, with the fractal dimension D = 2.1, indicating that the Pt nanoparticles form loose clusters inside the PVP solution, presumably due to the higher particle concentration. Using an ellipsoidal form factor for the shape of the Pt nanoparticles and the fractal model described previously to account for the aggregation effect, we can fit the SAXS

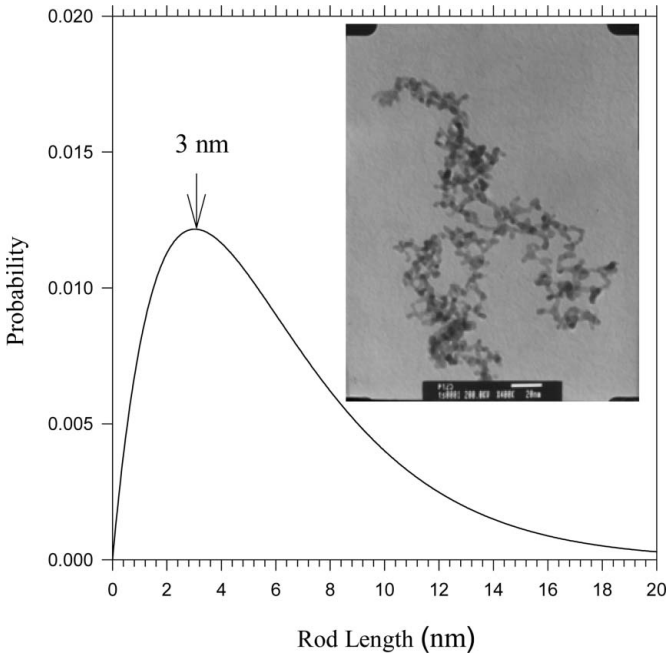

Figure 2
The Schultz distribution, with a most-probable rod length of 3 nm and a length polydispersity of 70%, is used in the rod-like model fitting for the SAXS data of the Pt nanoparticles shown in Fig. 2. The inset shows the TEM image of the Pt nanoparticles.

data well (the dashed curve). The parameters fitted are the fractal dimension D = 2.1 and the correlation length ξ = 30 nm for the aggregates, and the semi-major axis a = 2.3 nm and the semi-minor axis b = 1.3 nm for the ellipsoidal-like Pt nanoparticles. Except for the fractal aggregation effect, the dimensions of the Pt nanoparticles synthesized in the higher-concentration $PtCl_4$ solution is only marginally higher than that of the Pt nanoparticles synthesized previously in the solution with a much lower $PtCl_4$ concentration (1 mg ml^{-1}). With the comparable sizes in the two synthesis conditions, we conclude that the higher $PtCl_4$ concentration used in the synthesis contributes mainly to an increase of the number density of the Pt nanoparticles, leading to the clustering of the Pt nanoparticles.

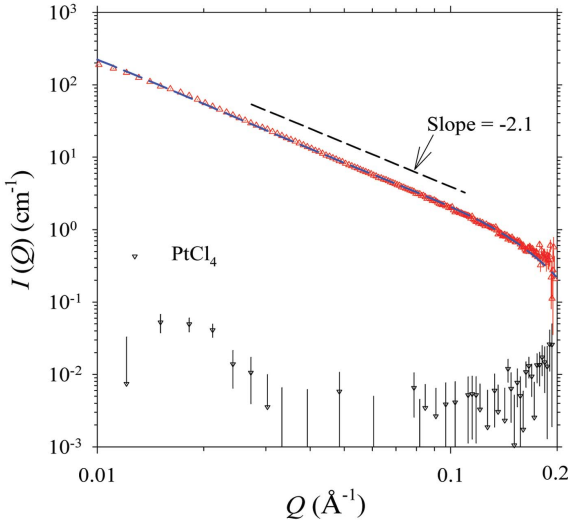

Figure 3
SAXS data for the Pt nanoparticles synthesized in the aqueous PVP solution with a high $PtCl_4$ concentration of 10 mg ml^{-1}. The data were fitted (dashed curve) with a fractal model and an ellipsoid form factor. The dashed line indicates the characteristic power law scattering $I(Q) \propto Q^{-D}$, with the fractal dimension D = 2.1. Also shown is the trivial scattering from the aqueous solution of 10 mg ml^{-1} $PtCl_4$.

4.3. Pt nanoparticles synthesized by PVP reduction

Fig. 4 shows the SAXS data for the aqueous solution of PVP/$PtCl_4$, without HCHO reduction agent, after the sample solution had been incubated at 323 K for 72 and 82 h. The prominent SAXS intensities measured, compared to those measured before annealing, reveal the existence of Pt nanoparticles in the solution. The results imply that Pt nanoparticles can be reduced by PVP, which has a weak reduction capability at 323 K. The power-law scattering characteristic observed (dashed line in Fig. 4), corresponding to a fractal dimension of 1.9, covers a relatively wide Q range up to $Q \simeq 0.2$ Å^{-1}. In the high-Q region, the lack of scattering features of the form factor of the Pt nanoparticles indicates that the size of the Pt nanoparticles synthesized must be smaller than ~1 nm, due to the fact that the scattering contribution from small nanoparticles (<1 nm) is essentially flat in the Q range studied (Freltoft *et al.*, 1986). From the Guinier approximation, we have also extracted a radius of gyration of 3.8 nm for the clusters of the Pt nanoparticles (corresponding to an overall size of ~10 nm for globular clusters). Both the particle size and the cluster size of the Pt nanoparticles reduced by PVP are significantly smaller those from the HCOH reduction shown previously.

Furthermore, the SAXS profile measured for the sample solution after 82 h annealing overlaps well with that measured after 72 h annealing after the higher intensity of the former has been scaled down by 1.2 times. The result implies a steady growth of the numbers of Pt nanoparticles and metal clusters, without growth of the particle size and the cluster size. The reduction and growth of the Pt nanoparticles seems to be controlled by the PVP chain density in the solution. It is likely that only the Pt metal ions that form polymer–metal ion complexes along the PVP chains can be reduced to metal atoms. Consequently, the size of the Pt nanoparticles is then limited to the space confined by PVP local chains of limited local metal-ion sources.

Using the same fractal model as that used previously, we can fit (dashed curves in Fig. 4) the two sets of data with a common fractal

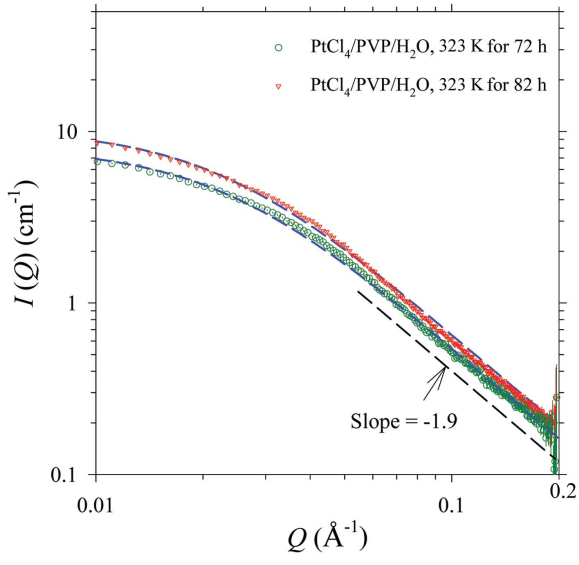

Figure 4
SAXS data for the aqueous solution of $PtCl_4$/PVP after 72 and 82 h annealing at 323 K.

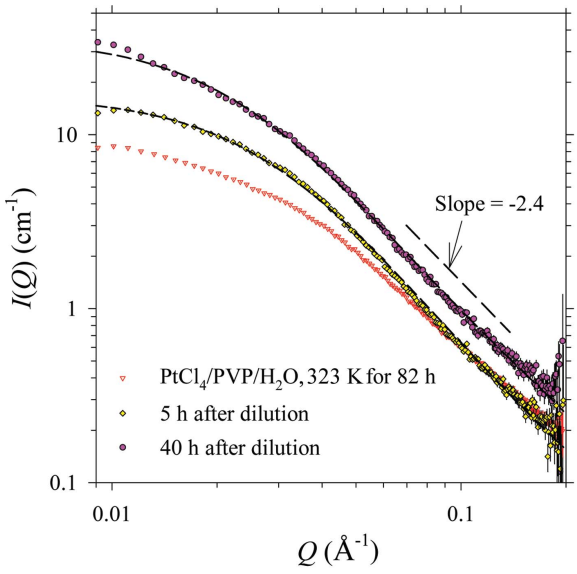

Figure 5
Concentration-normalized SAXS data for the annealed solution of $PtCl_4$/PVP at 323 K, measured 5 and 40 h after the sample dilution. Also shown are the SAXS data for the sample solution before concentration dilution.

dimension $D = 1.9 \pm 0.2$, a correlation length $\xi = 4.3 \pm 0.4$ nm, and a spherical form factor of diameter 0.6 ± 0.3 nm. The overall size $2\xi \simeq 9$ nm of the fractal domains of the Pt nanoparticles is consistent with that obtained from the Guinier approximation.

To further study the effect of PVP concentration on the growth and clustering behaviors of the Pt nanoparticles, we diluted the sample solution after 82 h annealing at 323 K to half of the initial PVP concentration. The concentration-normalized SAXS intensity distributions (Fig. 5) measured 5 and 40 h after the sample dilution indicate a new growth behavior of Pt nanoparticles differing from that observed before the sample dilution. From the steeper slopes of the SAXS profiles of the diluted sample solution, the Pt nanoparticles seem to form clusters of a denser packing (corresponding to a larger fractal dimension) in the sample solution of diluted PVP concentration. Using the same fractal model with a sphere form factor, we can adequately fit (dashed curves in Fig. 5) the two set of SAXS data measured 5 and 40 h after the sample dilution with correlation lengths $\xi = 3.5$ and 4.2 nm, sphere diameter $d = 1.2$ and 1.6 nm, and a common fractal dimension of $D = 2.4$. The result indicates that in the solution of diluted PVP concentration (lower local chain density of PVP), the Pt nanoparticles can grow further. As a consequence, the packing density (or fractal dimension) of Pt nanoparticles in the solution of PVP increases correspondingly. However, the fractal-like clusters maintain about the same size as that before dilution, indicating that the Pt metal cluster size may be confined by the overall PVP dimension (M_w = 10000) in the solutions during the PVP reduction process.

5. Conclusions

We have used SAXS to characterize the Pt nanoparticles synthesized in aqueous solutions of PVP/$PtCl_4$/HCHO and PVP/$PtCl_4$. With a high PVP/$PtCl_4$ weight ratio, the Pt nanoparticles synthesized can be characterized by short rod-like particles (~3 nm in length and 1 nm in radius). With a comparable PVP/$PtCl_4$ weight ratio, the Pt nanoparticles synthesized form clusters (~ 30 nm) of a fractal dimension of

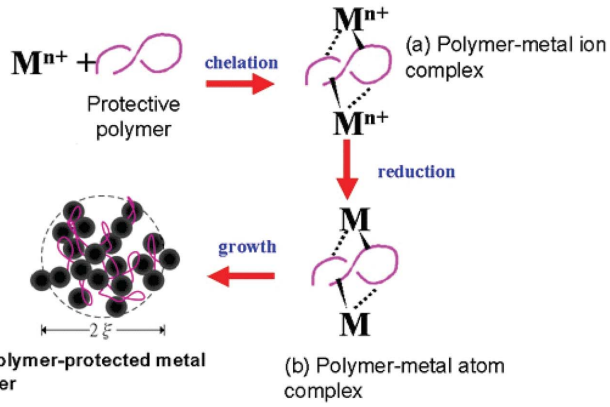

Figure 6
A route for the formation of the polymer–metal complex.

2.1, due to the higher number density of the nanoparticles in the solution. We have also demonstrated that Pt nanoparticles can also be synthesized by PVP at a medium temperature of 323 K, without the reduction agent HCHO. The particle size and clustering behaviors of the Pt nanoparticles reduced by PVP are closely related to the concentration of PVP in the solution. Nevertheless, both the Pt nanoparticles synthesized from the commonly used polyol process or the unusual PVP reduction form fractal-like clusters *via* association with the PVP chains whenever the number density of the particles is high enough. On the basis of the SAXS results, we assume a route for the formation of a polymer–metal cluster complex as shown in Fig. 6.

This research was supported by the National Science Council, ROC, grant Nos. NSC 94-2113-M-007-003 and NSC 95-2112-M-213-002, and the Ministry of Education, ROC, grant No. 91-I 0037-J4.

References

Camara, G. A., Giz, M. J., Paganin, V. A. & Ticianelli, E. A. (2002). *J. Electroanal. Chem.* **537**, 21–29.
Chen, S.-H. & Lin, T.-L. (1987). *Methods of Experimental Physics – Neutron Scattering in Condensed Matter Research*, edited by K. Skod and D. L. Price, Vol. 23B, ch. 16. New York: Academic Press.
Chen, S.-H. & Teixeira, J. (1986). *Phys. Rev. Lett.* **57**, 2583–2586.
Chen, W. X., Lee, J. M. & Liu, Z. (2002). *Chem. Commun.* pp. 2588–2589.
Freltoft, T., Kjems, J. K. & Sinha, S. K. (1986). *Phys. Rev. B*, **33**, 269–275.
Guo, X. H., Zhao, N. M., Chen, S. H. & Teixeira, J. (1990). *Biopolymers*, **29**, 335–346.
Hashimoto, T., Saijo, K., Harada, M. & Toshima, N. (1998). *J. Chem. Phys.* **109**, 5627–5638.
Higgins, J. S. & Benoit, H. C. (1994). *Polymer and Neutron Scattering*, p. 174. New York: Oxford University Press.
Hogarth, M. P. & Ralph, T. R. (2002). *Platinum Met. Rev.* **46**, 117–135.
Joo, S. H., Choi, S. J., Oh, I., Kwak, J., Liu, Z., Terasaki, O. & Ryoo, R. (2001). *Nature (London)*, **412**, 169–172.
Liu, R., Iddir, H., Fan, Q., Hou, G., Bo, A., Ley, K. L. & Smotkin, E. S. (2000). *J. Phys. Chem. B*, **104**, 3518–3531.
Mangin, Ph., Rodmacq, B. & Chamberod, A. (1985). *Phys. Rev. Lett.* **23**, 2899–2902.
Murphy, C. J. & Jana, N. R. (2002). *Adv. Mater.* **14**, 80–82.
Nam, J.-H., Jang, Y.-Y., Kwon, Y.-U. & Nam, J.-D. (2004). *Electrochem. Commun.* **6**, 737–741.
Schmidt, P. W. (1991). *J. Appl. Cryst.* **24**, 414–435.
Sheu, E. Y. (1992). *Phys. Rev. A*, **45**, 2428–2437.
Sun, Y. & Xia, Y. (2002). *Science*, **298**, 2176–2179.
Sun, Y., Yin, Y., Mayers, B. T., Herricks, T. & Xia, Y. (2002). *Chem. Mater.* **14**, 4736–4745.